Theoretical and experimental study of He free-jet expansions

L. Pedemonte, G. Bracco, and R. Tatarek*
Istituto Nazionale di Fisica della Materia and CFSBT-CNR, Dipartimento di Fisica, Via Dodecaneso 33, 16146 Genova, Italy
(Received 17 July 1998)

The paper reports on calculations of the flow properties in low-temperature He free-jet expansions by means of the Lennard-Jones potential and the recently appearing He-He van der Waals potential based on perturbation theory. The calculated speed ratios are compared with both the values we measured in the 20–80 K source temperature range and data which were already reported. The comparison points out a better agreement of our experimental results with the speed ratio values obtained by the recent potential whenever the parallel temperature of the beam decreases below 10^{-2} K. In the same temperature range the light He-cluster size is analyzed. [S1050-2947(99)01004-5]

PACS number(s): 34.20.Cf, 36.40.−c

In recent decades, highly expanded nozzle beams found a large number of important applications in molecular physics [1]. In particular, He is well suited to produce supersonic beams since its quantum properties lead to a higher centerline intensity and narrower velocity distribution than could be obtained with heavier gases [2]. These features recently enabled, for instance, a deeper insight into a large class of phenomena which occur on crystal surfaces at temperature close to melting, i.e., anharmonicity, surface diffusion, or roughening [3]. Therefore, the aim of this work is to explore the possibility of producing He-nozzle beams with extremely high energy resolution from both a theoretical and experimental point of view.

Until now, the evolution of the expanding He-beam velocity distribution was calculated at liquid nitrogen and room nozzle temperatures by Toennies *et al.* [2] assuming simple three parameter (12-6-8) potentials reverting back to the well-known Lennard-Jones (LJ) curve as a special case. Those authors found a good agreement with the experimental data collected at a nozzle temperature of 300 K for the LJ potential and the same result was obtained by Brusdeylins *et al.* [4] a few years later at 77 and 30 K. However, more refined potential models which attempt to account for the unique low-temperature behavior of helium and to reproduce a larger fraction of the experimental data (see, e.g., Ref. [5] for a historical review) are reported in the literature. In particular, a realistic He-He interaction potential must support a weakly bound dimer state whose detection [6], although questioned [7,8], was recently confirmed with nondestructive transmission diffraction experiments [9]. Among modern potentials, the van der Waals potential with Duman-Smirnov repulsive contribution derived from the perturbation theory by Tang, Toennies, and Yiu [10], hereafter called the TTY potential, satisfies the above requirement. Without any adjustable parameter, it agrees with recent *ab initio* results [11] as well as with quantum Monte Carlo calculations [5] and semiempirical potentials [12]. Moreover, it has a simple analytical form which allows a straightforward comparison with the available data.

*Author to whom correspondence should be addressed. FAX: +39 010 3622790. Electronic address: tatarek@fisica.unige.it

As far as we are aware, the TTY potential is used in this paper for the first time to calculate the evolution of He-flow properties during free-jet expansion in the source temperature and pressure ranges 20–80 K and 2–16 bars, respectively, in which the data were collected. Calculations performed with the LJ potential are also shown to enable a fruitful comparison with the present and previous data. Moreover, the size of the neutral He clusters appearing just before the dramatic decrease in the beam speed ratio is discussed.

To describe the He free-jet expansion, we solved the Boltzmann equation for the beam velocity distribution $f(\vec{v})$ using the theoretical method described in Refs. [13,14]. Briefly, the first basic assumption is to treat the expansion beyond the nozzle as spherically symmetric. Moreover, to take into account that the parallel and perpendicular velocity components with respect to the streamlines behave differently during the expansion, an ellipsoidal velocity distribution which consists of two Maxwellians with different temperatures (denoted, respectively, with $T_{\|}$ and $T_{\perp}$), i.e.,

$$f(\vec{v})=n\left(\frac{m}{2\pi k_b T_{\|}}\right)^{1/2}\left(\frac{m}{2\pi k_b T_{\perp}}\right) \times \exp\left(-\frac{m}{2k_bT_{\|}}(v_{\|}-u)^2-\frac{m}{2k_bT_{\perp}}v_{\perp}^2\right),$$

was assumed. Here m is the mass, n is the number density, and u is the average velocity of the expanding gas. We obtained the evolution of the parameters n, u, $T_{\|}$, and $T_{\perp}$ with the distance from the source x by solving numerically, using the standard Runge-Kutta computation procedure [15], a set of four coupled integro-differential equations deduced from the Boltzmann equation by the method of moments [2]. The integration begins at $r=x/d=2.5$ (d is the nozzle diameter), where the spherically symmetric model was found to be a good approximation [16]. The initial parameters were evaluated from the source conditions using the analytical formula of Ref. [17] for the isentropic expanding gas. To stop the expansion we checked the evolution of the ratio $b=T_{\perp}/T_{\|}$ from the initial value $b=1$, corresponding to equilibrium, through $b=0$ (corresponding to molecular flow) at $x/d \rightarrow\infty$. We assumed negligible collisional coupling at b

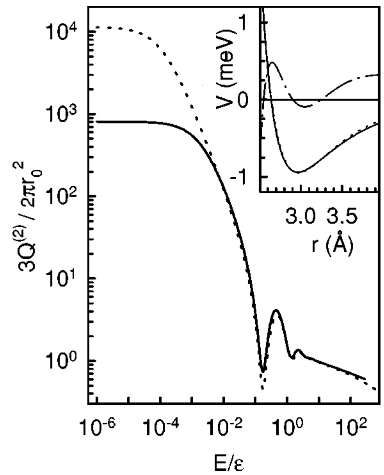

FIG. 1. The reduced viscosity cross section $3Q^{(2)}/2\pi r_0^2$ calculated for the LJ (—) and the TTY ($\cdots$) interatomic potential is plotted versus the reduced relative energy E/ϵ of the colliding atoms. Here r_0 is the zero of the intermolecular potential and ϵ is its well depth with values obtained from Ref. [20] and Ref. [10], respectively. The potential curves are compared in the inset where the dot-dashed line shows the difference between the TTY and LJ potential; the difference is multiplied by ten.

$\leqslant 0.01$ because the calculations up to $b=0.005$ produced no change in the flow parameters within a range less than 0.1%. The solution of the set of equations depends on the intermolecular forces between the expanding gas atoms through the collision integral

$$\Omega^{(2,1)}(T_{\rm eff})=\left(\frac{k_b T_{\rm eff}}{\pi m}\right)^{(1/2)}\int_0^\infty Q^{(2)}(E)\,\gamma^5\exp(-\gamma^2)\,d\gamma,$$

$$\gamma=\sqrt{\frac{E}{k_b T_{\rm eff}}}, \tag{1}$$

where $T_{\rm eff}$ is an effective average temperature varying between $T_\perp$ and $T_{||}$, $Q^{(2)}$ is the viscosity cross section, and E is the collision energy of two atoms in the center-of-mass system. We calculated the scattering cross section and the associated collision integral taking into account quantum effects which are quite important for He at temperatures below 10 K [18]. For collisions between Bose-Einstein particles,

$$Q^{(2)}(E)=\frac{8\pi\hbar^2}{mE}\sum_{l=0,2,4,\ldots}\frac{(l+1)(l+2)}{(2l+3)}\sin^2(\eta_{l+2}-\eta_l),$$

where η_l is the phase shift of the partial wave with orbital angular momentum l. Phase shifts were evaluated employing the standard computation procedure described in detail in Ref. [19] and the Runge-Kutta method [15] for the numerical integration of the Schrödinger equation. The He-He interaction is described by the LJ (12-6) [20] and the TTY [10] potentials whose shapes are compared in the inset of Fig. 1. Figure 1 shows the reduced viscosity cross section versus the reduced collision energy. According to the effective range theory, the remarkably large differences which can be noted in the $Q^{(2)}$ behavior, especially at the lowest energies, are directly related to the energy difference of the supported bound state [21]. The effect of different initial conditions (of

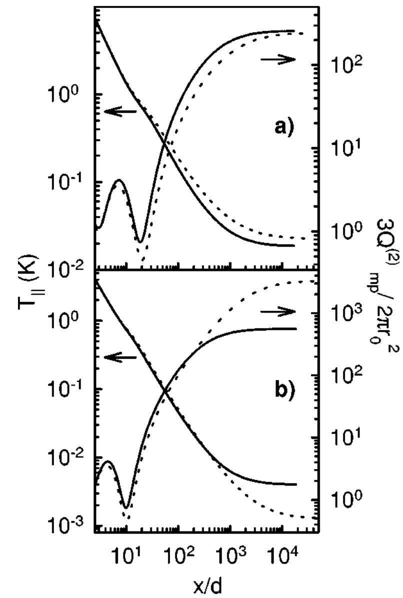

FIG. 2. The beam parallel temperature $T_{||}$ and the corresponding reduced most probable cross section $Q^{(2)}_{\rm mp}$ calculated for the LJ (—) and the TTY ($\cdots$) He-He potential are reported as a function of the distance x from the nozzle normalized with respect to its diameter d. The two panels correspond to different initial conditions for the beam expansion, i.e., different source temperature T_0 and pressure P_0: (a) $T_0=79$ K, $P_0=9$ bars; (b) $T_0=44$ K, $P_0=5$ bars.

the expanding beam) on the flow properties is investigated in the two panels of Fig. 2, where the evolution of the calculated parallel temperature and of the most probable cross section $Q^{(2)}_{\rm mp}$ with x/d are shown. $Q^{(2)}_{\rm mp}$ is defined as the value of $Q^{(2)}$ at $E_{\rm mp}=\frac{5}{2}k_b T_{\rm eff}$, which is the maximum of the weighting function in the collision integral [see Eq. (1), where we set $T_{\rm eff}=T_{||}$]. First, we note that for both potentials the minima in the cross sections are coupled to a shoulder in the $T_{||}$ behavior, i.e., to a drop in the temperature decrease rate, while the opposite is observed at the cross-section maxima. This suggests direct correlation between the local temperature and $Q^{(2)}$ despite the averaging over the relative velocity distribution in the collision integral. This correlation brings about the differences in the TTY and the LJ parallel temperature behavior. In fact, as long as the temperature of the expanding gas remains above $\sim 10^{-2}$ K, the TTY most probable cross-section curve is just below the LJ one leading to slightly greater $T_{||}$ values. That is what happens during the whole expansion described in panel (a). On the contrary, if $T_{||}$ decreases below 10^{-2} K (which corresponds to $E_{\rm mp}\sim 10^{-3}$ meV on the energy scale), as it happens in the final stages of the expansion described in panel (b), the TTY most probable cross section becomes remarkably higher than the LJ one leading to a supercooling of the TTY beam with respect to that described by the LJ potential.

To check the different behaviors of the parallel temperature pointed out by calculations, we performed measurements of the terminal velocity distribution in free-jet expansions with the He-atom beam line recently set up. Briefly, the beam particles leaving the high pressure, $P_0=2-16$ bars, low temperature, $T_0=22-79$ K, source through a $d=10$ μm nozzle are skimmed, chopped mechanically in short pulses of a few μs widths, and differentially pumped.

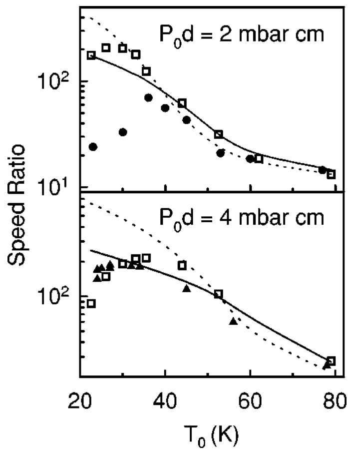

FIG. 3. The calculated LJ (—) and TTY (· · ·) terminal speed ratios of the expanding He beam are reported as a function of the source temperature T_0 at different P_0d values and compared with the values we measured (□). Repeated measurements at fixed source parameters give an estimation of the error bar falling within the symbols. The figure also reports the data from Ref. [23] and Ref. [24] represented with filled circles and triangles, respectively.

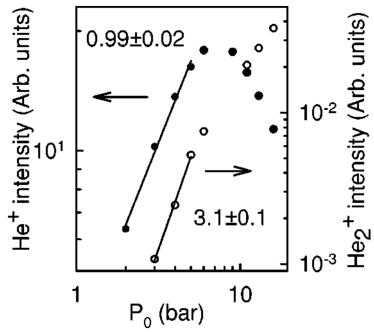

FIG. 4. He^+(●) and $He_2{}^+$(○) integrated intensities measured at $T_0=35.5$ K are reported versus the source pressure. The lines are least-square fits for data related to $P_0<6$ bars. See text for more details.

Thereafter, they are ionized by electron impact after an ~1.89 m flight path, mass analyzed, and detected. The nozzle-skimmer distance is 20 mm and T_0 is kept stable within 0.03 K during measurements.

More than 100 time-of-flight spectra were collected at different source parameters and analyzed to estimate the He-beam intensity I^+_{He} and the energy resolution. The analysis was performed fitting each spectrum by a constant, which accounts for the He background in the detector stage, and the ellipsoidal function converted into the time scale. This last was integrated to obtain the beam intensity while the contributions of the finite chopper opening time and the detector arrival time spreading were quadratically subtracted from its standard deviation to estimate the full width at half maximum of the beam, Δt_0 [22]. Finally, the measured speed ratio obtained as $S_{\mathrm{expt}}\sim1.65(t_0/\Delta t_0)$, where t_0 is the peak position, was compared with the theoretical value $S=\sqrt{\frac{1}{2}mu^2/(k_bT_{||})}$ calculated at $b=0.01$ for the considered potentials. Figure 3 reports the calculated LJ and TTY terminal speed ratios of the expanding beam as a function of the source temperature at $P_0d=2$ and 4 mbars cm together with our experimental data. The two P_0d values were chosen to compare our results with the data of Ref. [23] and Ref. [24]. First of all, the figure points out that all the data agree at the liquid nitrogen temperature. Moreover, the upper panel shows that, in going from the liquid nitrogen temperature until about 40 K, our results are more likely described by the LJ potential curve even though the LJ and TTY curves can hardly be distinguished in this temperature range. Thereafter, any further T_0 decrease makes our data follow the TTY predictions, thus overhanging the LJ expected values, until they collapse and strong deviations from both potentials appear. A similar behavior is also shown below about 50 K by the data we collected at $P_0d=4$ mbars cm. Although the observed speed ratio drop-off is a common feature to all the data reported in Fig. 3 and can be regarded as a clear indication of the onset of condensation, speed ratio values close to those predicted by the TTY potential are peculiar to our data alone. Now we can speculate the reason why speed ratios higher than predicted by the LJ potential were not observed before. The data from Ref. [23] show the beam parallel temperature $T_{||}$ cooled down to ~0.01 K at most. Therefore, the temperature range in which the cross sections differ largely was not explored in that case. On the contrary, the data from Ref. [24] do extend to $T_{||}\sim0.002$ K more likely following the LJ predictions. In the absence of any data analysis description, we can argue the crude data which were reported. In this case the speed ratio values are decreased with a larger effect on higher values, thus masking any deviation from the LJ potential.

To have a better understanding of the supersonic expansion in the low-temperature range, $T_{||}<0.01$ K, we searched for the presence of light He clusters in the beam setting the spectrometer at $m=8$ amu, thus looking for the He_2^+ signal. It is well known that this signal might appear for several reasons other than direct ionization of the dimer, including collision processes in the ionizer and ionization of large clusters followed by fragmentation [24]. Now, within a model similar to the sudden-freeze one [25], the ratio between the density of clusters of size N and the monomer density in the expanded beam behaves for monatomic gases as $\rho_N/\rho_1\propto P_0^{N-1}$, whenever the freezing temperature slowly depends on the source density [6,26]. Resting on this result, the He^+ and He_2^+ intensities measured at $T_0=35.5$ K are reported versus P_0 in the log-log plot of Fig. 4. Since on decreasing the source pressure below 6 bars the measured terminal parallel temperature of the beam remains constant within ±0.5 mK, the data in this pressure range were fitted with straight lines whose slopes resulted in 0.99 ± 0.02 and 3.1 ± 0.1 for the monomer and the dimer ion signal, respectively. This suggests that in the present case the He_2^+ signal arises from the helium trimer fragmentation in the electron impact ion source. A similar behavior was also observed in Refs. [27,28] at source temperatures 4.2 and 7 K, respectively. In the first case the authors could not identify the parent cluster while in the second case a trimer parent was suggested. Finally, our interpretation confirms the recent results of Schöllkopf and Toennies [9]. In that experiment, the fragile He_2 and He_3 clusters produced in the supersonic beam expansion were mass selected and nondestructively identified. Measuring the relative ionization and fragmentation probabilities, the authors concluded that at T_0

$=30$ K, $P_0=15$ bars the observed $He_2{}^+$ signal was mainly due to trimer fragmentation and they estimated the ratio $I_{He_2{}^+}/I_{He^+}$ to be about 1.8×10^{-2}, in excellent agreement with the value of $(1.8\pm0.2)\times10^{-2}$ we measured at 30 K, 16 bars.

Summarizing, we compared the He-nozzle beam speed ratios measured down to source temperatures of about 20 K with the calculated flow properties of the beam as derived both from the LJ and the more refined TTY interatomic potential. In particular, the TTY potential was proved to predict correctly the He-flow properties in the low-temperature range, i.e., whenever the beam parallel temperature decreases below 10^{-2} K. This was demonstrated to be largely due to the higher viscosity cross section at energies below ~1 μeV obtained for the TTY potential which correctly predicts the zero-energy resonance maximum in atomic collisions peculiar to the quantum He-He system. Finally, the size of the parent clusters producing the $He_2{}^+$ signal was studied. The data showed that the observed dimer intensity was mainly due to trimer fragmentation in the electron impact ion source.

The financial support from MURST through Grant No. 9702178261-003 is gratefully acknowledged.

[1] For a general review on nozzle beam applications, see, for instance, G. Scoles, *Atomics and Molecular Beam Methods*, edited by G. Scoles (Oxford University Press, New York, 1988), Vol. 1, pp. 3–13.
[2] J.P. Toennies and K. Winkelmann, J. Chem. Phys. **66**, 3965 (1977).
[3] J.F. Van der Veen and J.W.M. Frenken, Surf. Sci. **251/252**, 1 (1991).
[4] G. Brusdeylins, J.P. Toennies, and R. Vollmer, *Abstracts of XII International Symposium on Molecular Beams,* edited by V. Aquilanti (Perugia, Italy, 1989), p. 98.
[5] J.B. Anderson, C.A. Traynor, and B.M. Boghosian, J. Chem. Phys. **99**, 345 (1993).
[6] F. Luo, G.C. McBane, G. Kim, C.F. Giese, and W.R. Gentry, J. Chem. Phys. **98** 3564 (1993).
[7] E.S. Meyer, J.C. Mester, and I.F. Silvera J. Chem. Phys. **100**, 4023 (1994).
[8] F. Luo, G.C. McBane, G. Kim, C.F. Giese, and W.R. Gentry, J. Chem. Phys. **100**, 4023 (1994).
[9] W. Schöllkopf and J.P. Toennies, J. Chem. Phys. **104**, 1155 (1996); Science **266**, 1345 (1994).
[10] K.T. Tang, J.P. Toennies, and C.L. Yiu, Phys. Rev. Lett. **74**, 1546 (1995).
[11] B. Liu and A.D. McLean, J. Chem. Phys. **91**, 2348 (1989).
[12] R.A. Aziz and M.J. Slaman, J. Chem. Phys. **94**, 8047 (1991).
[13] E.L. Knuth and S.S. Fisher, J. Chem. Phys. **48**, 1674 (1968).
[14] D.R. Miller and R.P. Andres, *IV Symposium of Rarefied Gas Dynamics,* edited by L. Trilling and H.Y. Wachman (Academic, New York, 1969), Vol. 2, p. 1385.
[15] S.G. Mikhlin and K.L. Smolitsky, *Approximate Methods for Solution of Differential and Integral Equations*, edited by R. Bellman and R.E. Kalaba (American Elsevier, New York, 1967).
[16] H. Ashkenas and F.S. Sherman, *Vth Symposium of Rarefied Gas Dynamics*, edited by J.H. de Leeuw (Academic, New York, 1966), Vol. 2, p. 84.
[17] H. R. Murphy and D. R. Miller, J. Phys. Chem. **88**, 4474 (1984).
[18] S. Imam-Rahajoe, C.F. Curtiss, and R.B. Bernstein, J. Chem. Phys. **42**, 530 (1965).
[19] R.B. Bernstein, J. Chem. Phys. **33**, 795 (1960).
[20] J.P. Toennies, Chem. Phys. Lett. **20**, 238 (1973).
[21] J. Lekner, Mol. Phys. **23**, 19 (1972).
[22] D.M. Smilgies and J.P. Toennies, Rev. Sci. Instrum. **59**, 2185 (1988).
[23] K. Kern, R. David, and G. Comsa, Rev. Sci. Instrum. **56**, 369 (1985).
[24] H. Buchenau, E.L. Knuth, J. Northby, J.P. Toennies, and C. Winkler, J. Chem. Phys. **92**, 6875 (1990).
[25] D.R. Miller, *Atomics and Molecular Beam Methods*, edited by G. Scoles (Oxford University Press, New York, 1988), Vol. 1, p. 14.
[26] U. Buck, J. Phys. Chem. **92**, 1023 (1988); U. Buck and H. Meyer, J. Chem. Phys. **84**, 4854 (1986).
[27] P.W. Stephens and J.G. King, Phys. Rev. Lett. **51**, 1538 (1983).
[28] A.P.J. van Deursen and J. Reuss, J. Chem. Phys. **63**, 4559 (1975).